GENERALIZED FINITE ELEMENT METHOD ON THE LOCKING PROBLEM OF DEGENERATED 3-D TRIANGULAR SHELL ELEMENTS

Selma Hissae Shimura da Nóbrega
Departmento de Engenharia Mecânica, Universidade Federal do Rio Grande do Norte
Campus Universitário – 59072-970 – Natal, RN - Brazil
nobrega@ufrnet.br

Sergio Persival Baroncini Proença
Departamento de Engenharia de Estruturas, Escola de Engenharia de São Carlos, Universidade de São Paulo
Av. Trabalhador São-carlense,400 – 13566-590 – São Carlos, SP - Brazil
persival@sc.usp.br

Abstract. *In elastic linear analysis of thin shells, the locking phenomena are a frequent obstacle presented by the classic finite element simulation. In recent researches, one technique proposed to overcome locking phenomenon consists in a modification of the discrete potential energy by weighting differently the membrane and shear terms with respect to the bending terms. Another possibility derives from the use of the Generalized Finite Element Method (GFEM). One of its main features is the facility to provide a selective p refinement of the approximation on a certain region of the domain without compromising the element conformity. Such a feature is here explored as a base for a non conventional formulation of triangular shell elements free from locking. Then, both the mentioned alternative to lead with locking are combined, i.e., GFEM is applied over a formulation based on a modified potential energy functional. The numerical results are compared with those produced by classic FEM applied to structural analysis of plates and shells. Finally, some conclusions about the efficiency of proposed procedure as a numerical alternative to overcome locking in shell triangular elements are presented.*

Keywords*: Generalized Finite Element Method, Shells, Degenerated Elements, Locking*

1. Introduction

One numerical problem observed in the classic finite element analysis of thin plates and shells is known as locking. This can be detected when displacement-based formulations result in displacements much smaller than those expected by analytical solutions or those calculated with an appropriate formulation. In other words, the structure seems to present a false excessive rigidity that, obviously, is not the real one.

A great research effort has been undertaken during the last decades to overcome locking phenomena. One successful approach for quadrilateral shells elements with good predictive capabilities and a locking free behavior is the mixed formulation based on mixed interpolation of the tensorial components. However, for triangular shell elements it was not still possible to obtain the same level of accuracy displayed by quadrilateral elements.

In 1997, Bucalem and Nóbrega (1997) proposed one variation of the mixed formulation that consisted in a modification of the discrete potential energy by weighting differently the membrane and shear terms with respect to the bending terms. In their work an adaptation for the degenerated approach in the context of Naghdi shell theory was presented and the results for the triangular element with seven nodes and three tying points showed that this formulation needed further investigation.

Another possibility to suppress locking problems derives from the meshless method and is named as Generalized Finite Element Method (GFEM) proposed by Duarte, Babuska and Oden (2000). One of the main features of this method is the facility to provide selective p refinement of the approximation on a certain region of the domain without compromising the element conformity. Such a feature is explored in this work and also both the mentioned alternative are combined, i.e., GFEM is applied over a formulation based on a modified potential energy functional as a base for a non conventional formulation for triangular shell elements free from locking.

The present paper summarizes in Section 2 the mixed formulation for the degenerated solid approach. In Section 3, the main aspects of the Generalized Finite Element Method are presented. Numerical results obtained from the combination of these two techniques are compared with those produced by classic FEM and are included in Section 4. Finally, in Section 5, some conclusions about the efficiency of proposed procedure as a numerical alternative to overcome locking in shell triangular elements are presented.

2. Mixed formulation for the degenerated solid approach

The procedure presented in this section was studied by Bucalem and Nóbrega (1997) and was developed for the isoparametric shell element proposed by Ahmad, Irons and Zienkiewicz (1970). It consists in degeneration of a three-dimensional solid element and, for this reason, its geometry is represented by its midsurface, thickness and nodal direct vectors. The Fig. 1 shows a typical shell element with q nodes in its midsurface. Using the natural coordinates system

(*0,r,s,t*), the Cartesian coordinates (***x***) of any point in the element are described by the geometry interpolation. The *r* and *s* coordinates are positioned on the shell midsurface and *t* follows the direct vector ${}^{0}\boldsymbol{V}_n$.

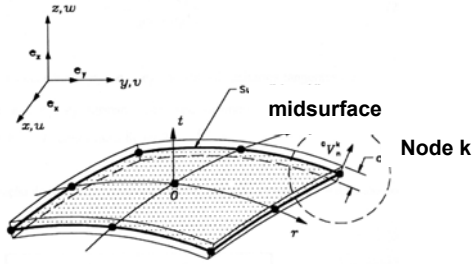

Figure 1. Generic shell finite element

The mixed formulation based on the modification of the discrete potential energy deals with Assumed Strain fields (***AS***), established by the definition of the Directly Interpolated strain fields (***DI***), so that it is possible to reduce the effects of membrane and shear locking in thin shell elements. Each different relation constructed between these parameters is related to a particular formulation. More details are described on Bucalem and Nóbrega (1997).

In order to introduce the idea of the modification of the potential energy in a degenerated solid approach formulation, it is necessary to define the assumed strain fields. Assuming small displacements and strains, the infinitesimal Green-Lagrange strain tensor can be written as

$$\boldsymbol{e} = \varepsilon_{rr}\left(\boldsymbol{g}^r \otimes \boldsymbol{g}^r\right) + \varepsilon_{ss}\left(\boldsymbol{g}^s \otimes \boldsymbol{g}^s\right) + \varepsilon_{rs}\left(\boldsymbol{g}^r \otimes \boldsymbol{g}^s + \boldsymbol{g}^s \otimes \boldsymbol{g}^r\right) + \varepsilon_{rt}\left(\boldsymbol{g}^r \otimes \boldsymbol{g}^t + \boldsymbol{g}^t \otimes \boldsymbol{g}^r\right) + \varepsilon_{st}\left(\boldsymbol{g}^s \otimes \boldsymbol{g}^t + \boldsymbol{g}^t \otimes \boldsymbol{g}^s\right) \tag{1}$$

where $\boldsymbol{e}_{ij}$ are the covariant components of the strain tensor and $\boldsymbol{g}^i \otimes \boldsymbol{g}^j$ is a tensorial covariant base formed by unity vectors associated to the isoparametric natural coordinates *r*, *s* and *t*.

Using the interpolations hypothesis for geometry and displacements we have

$$\varepsilon_{ij} = \left(\boldsymbol{B}_{ij0} + \boldsymbol{B}_{ij1}\right)\hat{\boldsymbol{u}} \quad , \qquad \varepsilon_{rt} = \boldsymbol{B}_{rtS}\,\hat{\boldsymbol{u}} \quad , \qquad \varepsilon_{st} = \boldsymbol{B}_{stS}\,\hat{\boldsymbol{u}} \tag{2}$$

where $\hat{\boldsymbol{u}}$ is the nodal degree of freedom vector, $\boldsymbol{B}_{ij0}$ and $\boldsymbol{B}_{ij1}$ produce, respectively, the membrane strain of the midsurface and the bending strain associated to nodal rotations, $\boldsymbol{B}_{rtS}$ and $\boldsymbol{B}_{stS}$, admitted constant through the thickness, are related to transverse shear strain. More detailed expressions for the $\boldsymbol{B}$ matrices are described in Nóbrega (1997).

Introducing Eq. (2) in Eq. (1) and considering the global tri-orthogonal coordinate system with base vectors $\boldsymbol{e}_x$, $\boldsymbol{e}_y$ and $\boldsymbol{e}_z$, the strain components can be written as

$$\begin{aligned}
\boldsymbol{e}_{mn} = {} & \left\{\left\{\boldsymbol{B}_{rr0}\left(\boldsymbol{e}_m\cdot\boldsymbol{g}^r\right)\left(\boldsymbol{g}^r\cdot\boldsymbol{e}_n\right) + \boldsymbol{B}_{ss0}\left(\boldsymbol{e}_m\cdot\boldsymbol{g}^s\right)\left(\boldsymbol{g}^s\cdot\boldsymbol{e}_n\right) + \boldsymbol{B}_{rs0}\left[\left(\boldsymbol{e}_m\cdot\boldsymbol{g}^r\right)\left(\boldsymbol{g}^s\cdot\boldsymbol{e}_n\right) + \left(\boldsymbol{e}_m\cdot\boldsymbol{g}^s\right)\left(\boldsymbol{g}^r\cdot\boldsymbol{e}_n\right)\right]\right\} + \right. \\
& + \left\{\boldsymbol{B}_{rr1}\left(\boldsymbol{e}_m\cdot\boldsymbol{g}^r\right)\left(\boldsymbol{g}^r\cdot\boldsymbol{e}_n\right) + \boldsymbol{B}_{ss1}\left(\boldsymbol{e}_m\cdot\boldsymbol{g}^s\right)\left(\boldsymbol{g}^s\cdot\boldsymbol{e}_n\right) + \boldsymbol{B}_{rs1}\left[\left(\boldsymbol{e}_m\cdot\boldsymbol{g}^r\right)\left(\boldsymbol{g}^s\cdot\boldsymbol{e}_n\right) + \left(\boldsymbol{e}_m\cdot\boldsymbol{g}^s\right)\left(\boldsymbol{g}^r\cdot\boldsymbol{e}_n\right)\right]\right\} + \\
& \left. + \left\{\boldsymbol{B}_{rtS}\left[\left(\boldsymbol{e}_m\cdot\boldsymbol{g}^r\right)\left(\boldsymbol{g}^t\cdot\boldsymbol{e}_n\right) + \left(\boldsymbol{e}_m\cdot\boldsymbol{g}^t\right)\left(\boldsymbol{g}^r\cdot\boldsymbol{e}_n\right)\right] + \boldsymbol{B}_{stS}\left[\left(\boldsymbol{e}_m\cdot\boldsymbol{g}^s\right)\left(\boldsymbol{g}^t\cdot\boldsymbol{e}_n\right) + \left(\boldsymbol{e}_m\cdot\boldsymbol{g}^t\right)\left(\boldsymbol{g}^s\cdot\boldsymbol{e}_n\right)\right]\right\}\right\}\hat{\boldsymbol{u}}
\end{aligned} \tag{3}$$

It is possible to identify the following three matrices $\boldsymbol{B}_{0mn}$, $\boldsymbol{B}_{1mn}$ and $\boldsymbol{B}_{Smn}$ from Eq. (3)

$$\boldsymbol{B}_{0mn} = \boldsymbol{B}_{rr0}\left(\boldsymbol{e}_m\cdot\boldsymbol{g}^r\right)\left(\boldsymbol{g}^r\cdot\boldsymbol{e}_n\right) + \boldsymbol{B}_{ss0}\left(\boldsymbol{e}_m\cdot\boldsymbol{g}^s\right)\left(\boldsymbol{g}^s\cdot\boldsymbol{e}_n\right) + \boldsymbol{B}_{rs0}\left[\left(\boldsymbol{e}_m\cdot\boldsymbol{g}^r\right)\left(\boldsymbol{g}^s\cdot\boldsymbol{e}_n\right) + \left(\boldsymbol{e}_m\cdot\boldsymbol{g}^s\right)\left(\boldsymbol{g}^r\cdot\boldsymbol{e}_n\right)\right]$$

$$\boldsymbol{B}_{1mn} = \boldsymbol{B}_{rr1}\left(\boldsymbol{e}_m\cdot\boldsymbol{g}^r\right)\left(\boldsymbol{g}^r\cdot\boldsymbol{e}_n\right) + \boldsymbol{B}_{ss1}\left(\boldsymbol{e}_m\cdot\boldsymbol{g}^s\right)\left(\boldsymbol{g}^s\cdot\boldsymbol{e}_n\right) + \boldsymbol{B}_{rs1}\left[\left(\boldsymbol{e}_m\cdot\boldsymbol{g}^r\right)\left(\boldsymbol{g}^s\cdot\boldsymbol{e}_n\right) + \left(\boldsymbol{e}_m\cdot\boldsymbol{g}^s\right)\left(\boldsymbol{g}^r\cdot\boldsymbol{e}_n\right)\right]$$

$$\boldsymbol{B}_{Smn} = \boldsymbol{B}_{rtS}\left[\left(\boldsymbol{e}_m\cdot\boldsymbol{g}^r\right)\left(\boldsymbol{g}^t\cdot\boldsymbol{e}_n\right) + \left(\boldsymbol{e}_m\cdot\boldsymbol{g}^t\right)\left(\boldsymbol{g}^r\cdot\boldsymbol{e}_n\right)\right] + \boldsymbol{B}_{stS}\left[\left(\boldsymbol{e}_m\cdot\boldsymbol{g}^s\right)\left(\boldsymbol{g}^t\cdot\boldsymbol{e}_n\right) + \left(\boldsymbol{e}_m\cdot\boldsymbol{g}^t\right)\left(\boldsymbol{g}^s\cdot\boldsymbol{e}_n\right)\right]$$

The linear strain tensor is obtained as

$$\boldsymbol{e} = \begin{bmatrix} \varepsilon_{xx} \\ \varepsilon_{yy} \\ \varepsilon_{zz} \\ 2\varepsilon_{xy} \\ 2\varepsilon_{xz} \\ 2\varepsilon_{yz} \end{bmatrix} = \begin{bmatrix} \boldsymbol{B}_{0xx} + \boldsymbol{B}_{1xx} + \boldsymbol{B}_{Sxx} \\ \boldsymbol{B}_{0yy} + \boldsymbol{B}_{1yy} + \boldsymbol{B}_{Syy} \\ \boldsymbol{B}_{0zz} + \boldsymbol{B}_{1zz} + \boldsymbol{B}_{Szz} \\ \boldsymbol{B}_{0xy} + \boldsymbol{B}_{1xy} + \boldsymbol{B}_{Sxy} \\ \boldsymbol{B}_{0xz} + \boldsymbol{B}_{1xz} + \boldsymbol{B}_{Sxz} \\ \boldsymbol{B}_{0yz} + \boldsymbol{B}_{1yz} + \boldsymbol{B}_{Syz} \end{bmatrix} \hat{\boldsymbol{u}} = \left(\boldsymbol{B}_0 + \boldsymbol{B}_1 + \boldsymbol{B}_S \right) \hat{\boldsymbol{u}} \tag{4}$$

The stiffness matrix of the element for the displacement-based formulation is expressed as

$$\boldsymbol{K}^e = \int_{0_V} \left(\boldsymbol{B}_0 + \boldsymbol{B}_1 + \boldsymbol{B}_S \right)^T \boldsymbol{C} \left(\boldsymbol{B}_0 + \boldsymbol{B}_1 + \boldsymbol{B}_S \right) d^0V \tag{5}$$

where the constitutive matrix $\boldsymbol{C}$ is defined for a global coordinate system and obtained by the transformation of an original constitutive matrix established for a local system.

For the mixed formulation, the assumed covariant strain field (***AS***) is defined in n_{ij} tying points which natural coordinates are given by $\boldsymbol{r}_k$, $\boldsymbol{s}_k$ and $\boldsymbol{t}$.

$$\boldsymbol{e}_{ij}^{AS}(\boldsymbol{r},\boldsymbol{s},\boldsymbol{t}) = \sum_{k=1}^{n_{ij}} \boldsymbol{h}_k^{ij}(\boldsymbol{r},\boldsymbol{s})\, \boldsymbol{e}_{ij}^{DI}(\boldsymbol{r}_k,\boldsymbol{s}_k,\boldsymbol{t}) \tag{6}$$

Note that $\boldsymbol{e}_{ij}^{DI}$ represents the directly interpolated covariant strain component. Since $\boldsymbol{e}_{ij}^{DI} = \boldsymbol{B}_{ij}^{DI}\, \hat{\boldsymbol{u}}$, then $\boldsymbol{e}_{ij}^{AS} = \boldsymbol{B}_{ij}^{AS}\, \hat{\boldsymbol{u}}$. Comparing with Eq. (7), we have

$$\boldsymbol{B}_{ij0}^{AS} = \sum_{k=1}^{n_{ij}} \boldsymbol{h}_k^{ij}(\boldsymbol{r},\boldsymbol{s})\, \boldsymbol{B}_{ij0}^{DI}(\boldsymbol{r}_k,\boldsymbol{s}_k,\boldsymbol{t}), \qquad \boldsymbol{B}_{rtS}^{AS} = \sum_{k=1}^{n_{ij}} \boldsymbol{h}_k^{ij}(\boldsymbol{r},\boldsymbol{s})\, \boldsymbol{B}_{rtS}^{DI}(\boldsymbol{r}_k,\boldsymbol{s}_k,\boldsymbol{t}), \qquad \boldsymbol{B}_{stS}^{AS} = \sum_{k=1}^{n_{ij}} \boldsymbol{h}_k^{ij}(\boldsymbol{r},\boldsymbol{s})\, \boldsymbol{B}_{stS}^{DI}(\boldsymbol{r}_k,\boldsymbol{s}_k,\boldsymbol{t}) \tag{7}$$

All the directly interpolated $\boldsymbol{B}^{DI}$ matrices in Eq. (7) correspond to the displacement-based formulation ones and were described earlier in Eq. (2). Also, the matrices $\boldsymbol{B}_0^{AS}$ and $\boldsymbol{B}_S^{AS}$ are those defined in Eq. (3) for each occurrence of $\boldsymbol{B}_{ij0}$, $\boldsymbol{B}_{rtS}$ and $\boldsymbol{B}_{stS}$.

It is important, at this point, to comment about the mixed formulation proposed by Arnold and Brezzi (1993) in the context of Naghdi theory. It can be obtained from the minimization of the following functional

$$\boldsymbol{\Pi}^M = \frac{1}{2}\left\{ \boldsymbol{E}_B + c_0 a^2 \boldsymbol{E}_S^{DI} + \left(1 - c_0 a^2 \right) \boldsymbol{E}_S^{AS} + c_0 a^2 \boldsymbol{E}_M^{DI} + \left(1 - c_0 a^2 \right) \boldsymbol{E}_M^{AS} \right\} + \boldsymbol{P} \tag{8}$$

where $\boldsymbol{E}_B$ is the strain energy caused by bending effects; $\boldsymbol{E}_S^{DI}$ and $\boldsymbol{E}_S^{AS}$, occur because of the transverse shear action; and $\boldsymbol{E}_M^{DI}$ and $\boldsymbol{E}_M^{AS}$, because of membrane action. The coefficient c_0 is defined as the reciprocal of the area of the midsurface of the shell and the thickness is *a*.

The mixed formulation applied to shell model and based on the degeneration concept uses a strain energy partition in a similar way as presented in Eq. (8). The stiffness matrix of the element is determined as

$$\mathbf{K}^e = \mathbf{K}_B^{DI} + \mathbf{K}_{BMS}^{DI} + c_0 a^2 \left(\mathbf{K}_S^{DI} + \mathbf{K}_{MS}^{DI} \right) + \left(1 - c_0 a^2 \right) \left(\mathbf{K}_S^{AS} + \mathbf{K}_{MS}^{AS} \right) \tag{9}$$

It is possible to identify the matrices that correspond to membrane (M), transverse shear (S) and bending (B) behaviors which can lead to the corresponding strain energy terms. The matrices in Eq. (10) can be defined

$$\boldsymbol{K}_B^{DI} = \int_{0_V} \left(\boldsymbol{B}_1^{DI^T} \boldsymbol{C} \boldsymbol{B}_1^{DI} \right) d^0V \tag{10a}$$

$$\boldsymbol{K}_{BMS}^{DI} = \int_{0_V} \left[\left(\boldsymbol{B}_0^{DI^T} \boldsymbol{C} \boldsymbol{B}_1^{DI} \right) + \left(\boldsymbol{B}_1^{DI^T} \boldsymbol{C} \boldsymbol{B}_0^{DI} \right) + \left(\boldsymbol{B}_1^{DI^T} \boldsymbol{C} \boldsymbol{B}_S^{DI} \right) + \left(\boldsymbol{B}_S^{DI^T} \boldsymbol{C} \boldsymbol{B}_1^{DI} \right) \right] d^0V \tag{10b}$$

$$\boldsymbol{K}_S^{DI} = \int_{0_V} \left(\boldsymbol{B}_S^{DI^T} \boldsymbol{C} \boldsymbol{B}_S^{DI} \right) d^0V \tag{10c}$$

$$\boldsymbol{K}_S^{AS} = \int_{0_V} \left(\boldsymbol{B}_S^{AS^T} \boldsymbol{C} \boldsymbol{B}_S^{AS} \right) d^0V \tag{10d}$$

$$\boldsymbol{K}_{MS}^{DI} = \int_{0_V} \left[\left(\boldsymbol{B}_0^{DI^T} \boldsymbol{C} \boldsymbol{B}_0^{DI} \right) + \left(\boldsymbol{B}_0^{DI^T} \boldsymbol{C} \boldsymbol{B}_S^{DI} \right) + \left(\boldsymbol{B}_S^{DI^T} \boldsymbol{C} \boldsymbol{B}_0^{DI} \right) \right] d^0V \tag{10e}$$

$$\boldsymbol{K}_{MS}^{AS} = \int_{0_V} \left[\left(\boldsymbol{B}_0^{AS^T} \boldsymbol{C} \boldsymbol{B}_0^{AS} \right) + \left(\boldsymbol{B}_0^{AS^T} \boldsymbol{C} \boldsymbol{B}_S^{AS} \right) + \left(\boldsymbol{B}_S^{AS^T} \boldsymbol{C} \boldsymbol{B}_0^{AS} \right) \right] d^0V \tag{10f}$$

For all numerical simulations presented in this work, the triangular shell element was constructed with three Gauss points for the membrane and transverse shear strain, and seven Gauss points for the directly interpolated strain.

3. Generalized finite element method

The Generalized Finite Element Method has some interesting aspects to be considered during the implementation phase of the code. They are, for example, the possibility to *(a)* construct the space of enrichment functions with polynomial and harmonic functions or functions that represents the analytical solution of the problem; *(b)* suppress some inconvenient that can occur when the domain of the shape functions is associated to the mesh; and *(c)* preserve, essentially, the same implementation of the classic MEF code. The basic ideas of GFEM are described in Duarte, Babuska and Oden (2000) considering one-dimensional linear finite element and are reproduced in this work.

Consider a local circular domain Ω_α with center at node α, and called "support" or "cloud". The union of the supports defined in each node of the domain results in an open covering $\overline{\Omega}$ that contains the Ω domain

$$\overline{\Omega} \subset \bigcup_{\alpha=1}^{N} \Omega_\alpha \tag{11}$$

where N is the number of local supports. The base function φ_α is established for each support and denotes a linear finite element partition of unity. The GFEM function F_α is obtained in each node multiplying the base functions φ_α and Q_α functions.

$$F_\alpha = \varphi_\alpha \; Q_\alpha \tag{12}$$

The local space Q_α can be generated considering a tensor product of polynomials or a complete set of polynomial basis. For the bi-dimensional problems presented in this paper, we have

1) if Q_α is obtained from a tensor product of polynomials

$$\overline{Q}_\alpha^p = \left\{ L_{ij}(\bar{x}) : 0 \le i,j \le p, i,j \ge 0, \; p \ge 0 \right\} \tag{13}$$

2) if Q_α is taken from a complete set of polynomials

$$\hat{Q}_\alpha^p = \left\{ L_{ij}(\bar{x}) \,\middle|\, 0 \le i,j \le p, 0 \le i + j \le p \right\} \tag{14}$$

The global approximation space Q is constructed with local spaces presented in Eqs. (13) or (14) as $Q = span\left\{F_N^p\right\}$ and is composed by sets of polynomials of degree $g \le p$. Introducing the enrichment techniques in the degenerated shell finite element formulation, for each integration point (*i*), the displacement filed approximation are

$$\boldsymbol{u} = \sum_{\alpha=1}^{N} \sum_{k=1}^{q} \psi_k^{\alpha}(r_i, s_i)\, \boldsymbol{u}_k + \frac{t}{2} \sum_{\alpha=1}^{N} \sum_{k=1}^{q} \boldsymbol{a}_k\, \psi_k^{\alpha}(r_i, s_i) \left(-\alpha_k\, \boldsymbol{V}_2^k + \beta_k\, \boldsymbol{V}_1^k\right) \tag{15}$$

where N is the number of the vertices and q is the element node number.

As previously affirmed, the structure of the classic finite element code is preserved and the basic difference is the definition of the shape functions. The narrow band of the stiffness matrix is maintained although its order increases with the number of new parameters introduced during the enrichment phase. In order to eliminate linear dependencies on the stiffness matrix resulting from GFEM, the iterative procedure proposed by Babuska, Strouboulis e Copps and described by Duarte, Babuska and Oden (2000) was implemented in the code.

4. Numerical results

Benchmarks tests like:1) Cook panel, 2) simply supported square plate, 3) clamped square plate, both under concentrated load, and 4) curved cantilever are analyzed in order to provide a validation of the proposed formulation. The results are obtained considering or not the nodal enrichment. This enrichment is applied in all internal nodes of the domain and only for the membrane displacements.

The following formulations were considered: *a)* classical FEM; *b)* classical FEM with nodal enrichment (GFEM); *c)* mixed formulation based on the modification of the potential energy (MM – **M**ixed **M**ethod); and *d)* mixed formulation based on the modification of the potential energy with nodal enrichment (GMM – **G**eneralized **M**ixed **M**ethod).

The enrichment functions adopted in all simulations are the linear polynomials (P1), quadratic polynomials (P2) and spline functions (SP)

P1: $1 + x + y$, P2: $1 + x + y + x^2 + xy + y^2$, SP: $2x^3 + 2y^3 + 6x^2y + 6xy^2 - 3x^2 - 3y^2 - 6xy + 1$

4.1 Curved cantilever

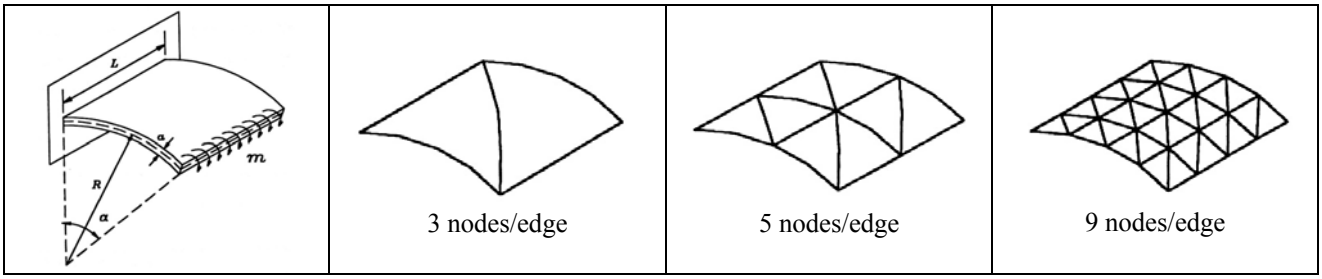

Figure 2. Curved cantilever model and mesh refinement

The curved cantilever problem under pure bending load is illustrated in Fig. 2. The geometric and material data are: thickness = 0.2 m; R = 2m; $\alpha = 30^o$; E = 100 kN/m^2; L = 1 m; and m = 240 kN.m/m. The capability of the triangular shell finite element in modeling curved surfaces is analyzed when this benchmark test is used. The meshes adopted are described in Fig. 2 and the results obtained for the rotation of the cantilever tip are presented in Figs. 3 to 4 considering the analytical solution equal to 1.7951958×10^{-2}.

Figures 3 and 4 show the approximated response obtained with 16 Gauss points in the integration process. Nóbrega and Proença (2004) discussed the influence of the number of Gauss point adopted in the response performance and 16 points or more were recommended for all analysis related to this research.

Observing the lateral scale limits for the normalized response in both figures, we can see that for classic FEM the results lock but, apparently, converge to the analytical solution with mesh refinement. In GFEM analysis the approximations are more flexible but still lock for a poor mesh. The responses for MM and GMM analysis in Fig. 4 are similar and do not suffer from this numerical difficult.

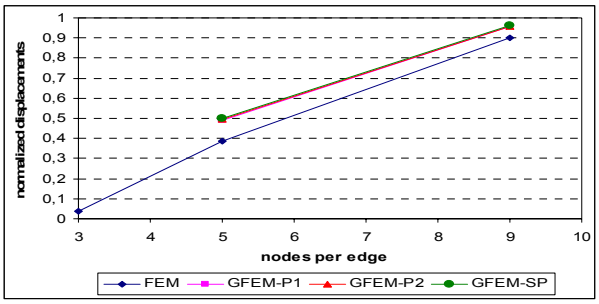

Figure 3. FEM x GFEM – *thickness/edge* = 1/100.

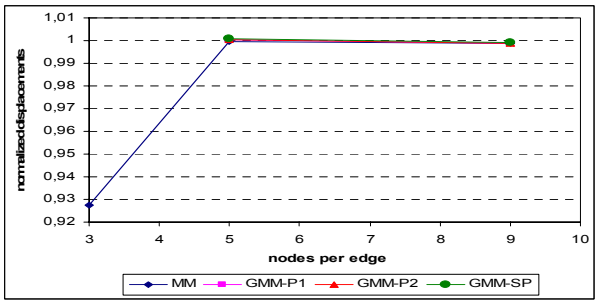

Figure 4. MM x GMM – *thickness/edge* = 1/100.

Figures 5 and 6 illustrate the MM and GMM curves for a thick and thin curved cantilever with thickness per edge dimension ratio equals to 1/10 and 1/1000, respectively. In both cases the performance for the proposed formulation is very satisfactory.

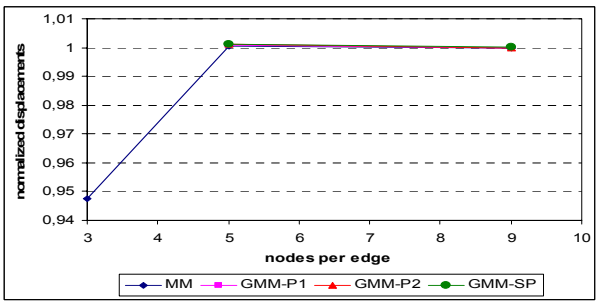

Figure 5. MM x GMM – *thickness/edge* = 1/10.

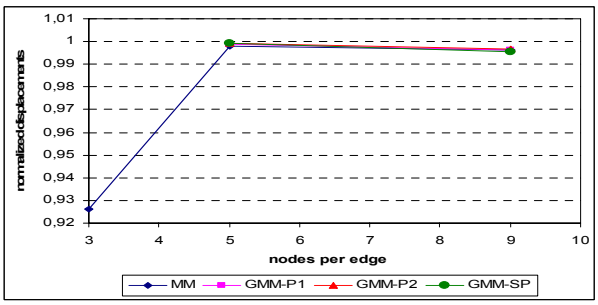

Figure 6. MM x GMM – *thickness/edge* = 1/1000.

4.2 Simply supported square plate

This problem refers to a square plate (1 m x 1 m) and thickness equal to 0.01 m (thickness/edge dimension ratio = 1/100). Young modulus (E) is equal to 2.1×10^8 kN/m^2 and Poisson coefficient to 0.3. The concentrated load applied on its center node is 100 kN and the analytical solution for the displacement on central node is 0.6023 m, as described by Timoshenko and Krieger (1959).

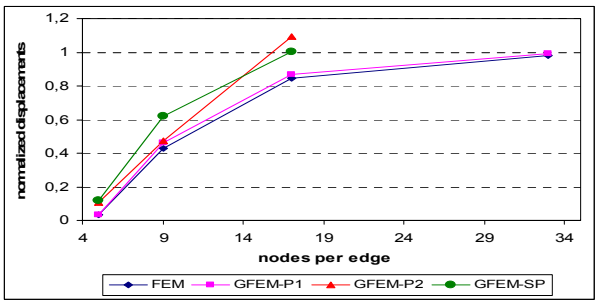

Figure 7. FEM x GFEM – *thickness/edge* = 1/100.

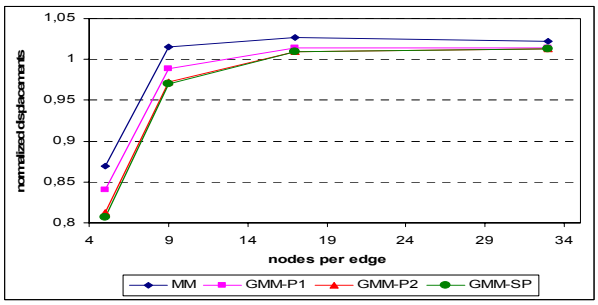

Figure 8. MM x GMM – *thickness/edge* = 1/100.

Figure 7 shows that better results are attained when using P1 enrichment functions but they still lock. Fig. 8 indicates that the MM formulation reduces locking and the nodal enrichment provides less flexible response. In this case, P1 enrichment function produces a better approximation that converges to the analytical solution with progressive refinement.

In Figs. 9 and 10 illustrate curves for thickness/edge dimension ratio = 1/10 and 1/1000, respectively. Fig. 9 shows that for thick plates the results due to the mixed formulation are more flexible than those obtained with nodal enrichment. In this case, the analytical solution can be used only as a reference value because it was calculated for thin plate situations. In Fig. 10, for a very thin plate the mixed formulation curve presents a satisfactory behavior and the enrichment of the membrane term is not so effective.

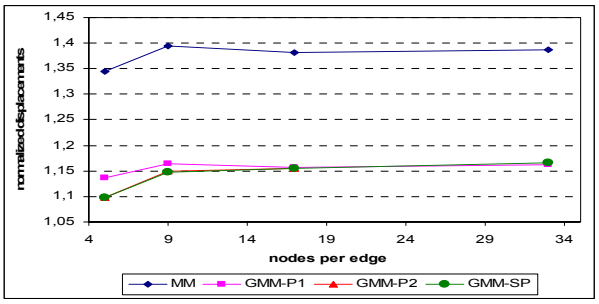

Figure 9. MM x GMM – *thickness/edge* = 1/10.

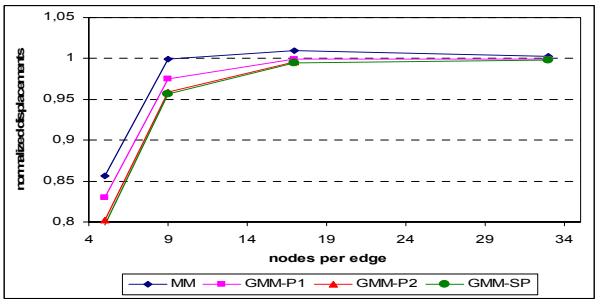

Figure 10. MM x GMM – *thickness/edge* = 1/1000.

4.3 Clamped square plate

Material properties, geometry and loading are similar to those described for simply supported plate. Figs. 11 and 12 show the normalized results based on the value equal to 0,2912 m, obtained from Timoshenko and Krieger (1959).

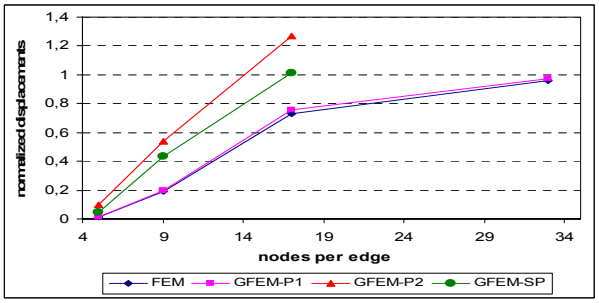

Figure 11. MEF x MEFG – *thickness/edge* = 1/100.

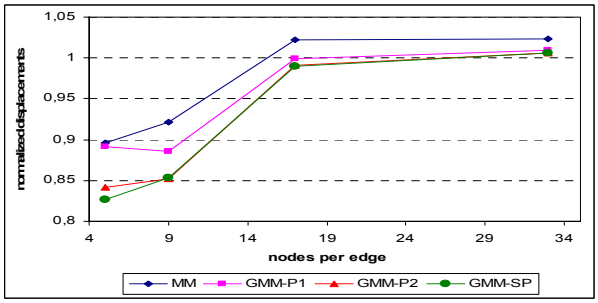

Figure 12. MM x MMG – *thickness/edge* = 1/100.

Again, FEM and GFEM approximations (Fig. 11) suffer from locking and the rigid responses tend to the analytical solution with the increase of the refinement. For MM and GMM formulation (Fig. 12), results are less affected by locking. The observations about the performance exhibited in Figs.13 and 14 are the same of those referenced for simply supported plate. The curve for MM formulation in Fig. 14 is sufficiently precise.

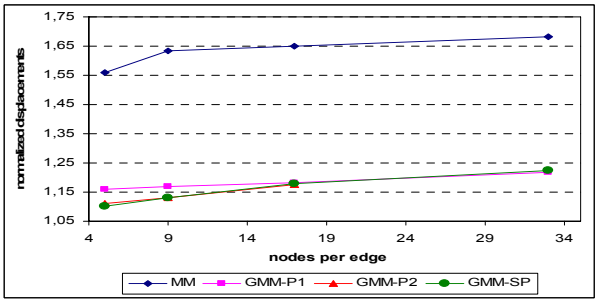

Figure 13. MM x MMG – *thickness/edge* = 1/10.

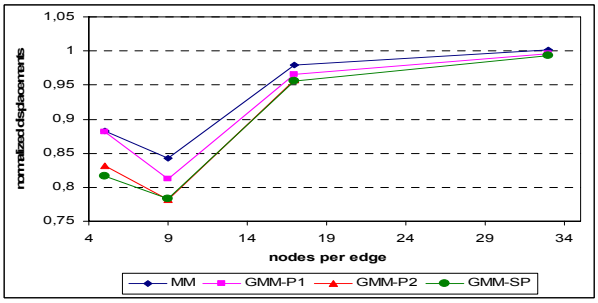

Figure 14. MM x MMG – *thickness/edge* = 1/1000.

4.4 Cook panel

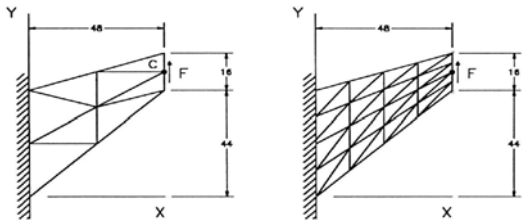

Thickness = 0.01 m

$E = 100$ kN/m^2

$\nu = 0.3$

$F = 0.01$ kN

Figure 15. Cook panel mesh (units in cm)

This is a plane stress problem and the analytical solution for the displacement on node C, as described by Cook (1987), is 0.239 m. Normalized by the analytical solution, the results obtained for a thickness/major dimension ratio equal 1/100 are listed on Tab.1 and Tab. 2.

Table 1 show that FEM approximations are rigid but converge to the analytical solution with mesh refinement. The use of P1, P2 and SP enrichment function in GFEM formulation makes the response more flexible, and it is still

possible to verify that satisfactory results are obtained for poor meshes, for example, for a 9 node/edge mesh and P2 enrichment function the response is close to that calculated for a 17 node/edge mesh in FEM (P0 enrichment).

In Tab. 2 the responses are flexible and converge to the analytical solution with mesh refinement. The enrichment of membrane terms does not affect the results.

Table 1. Node C displacement for FEM and GFEM.

	5 nodes/edge	9 nodes/ edge	17 nodes/edge
P0	0.2360	0.2389	0.2395
P1	0.2367	0.2391	0.2395
P2	0.2372	0.2393	0.2395
SP	0.2375	0.2394	0.2395

Table 2. Node C displacement for MM and GMM.

	5 nodes/ edge	9 nodes/ edge	17 nodes/ edge
P0	0.3219	0.2621	0.2454
P1	0.3226	0.2623	0.2454
P2	0.3228	0.2623	0.2454
SP	0.3235	0.2624	0.2454

Note: Pi indicates a polynomial enrichment function with degree i; and SP a spline function

5. Conclusion

This paper deals with a non-conventional shell finite element formulation which mathematical basis consists in a union of two procedures: a mixed formulation with modification of the potential energy and nodal enrichment promoted by GFEM. The idea is to combine their main qualities to obtain a triangular shell finite element free from locking.

Initially, a comment about the results obtained for classic FEM and mixed formulation (MM) is presented. As it was expected, the rigid responses of FEM formulation show the influence of locking. On the other side, the MM diminishes the locking effects but converges to a flexible value when compared to the analytical solution.

The performance of the approximations for both procedures is improved with nodal enrichment. It is clearly verified in plate simulations: FEM responses are transformed to more flexible ones and, for MM, they became rigid so that for a poor mesh it is possible to verify a satisfactory behavior. Another aspect is related to the enrichment function. The spline function is ideal for analysis involving shell structures because improve in a significantly the formulation performance.

Considering the curved cantilever problem, the MM and GMM response are very close and rapidly converges to the analytical solution. In fact, the enrichment technique does not affect the MM solution. It is recommended, for this problem, a simulation considering a more refined mesh to really observe the performance of the proposed formulation.

As a final remark, the combination of the mixed formulation with a modification of the potential energy and the nodal enrichment technique provides satisfactory results for the analyzed benchmark-tests and confirm the viability of the triangular shell formulation in study. Of course, other benchmarks like those involving single and double curvature must be tested in order to complete this conclusion.

6. Acknowledgements

The author S. H. S Nóbrega thanks UFRN – Universidade Federal do Rio Grande do Norte and CNPq - Conselho Nacional de Desenvolvimento Científico e Tecnológico for financial support.

7. References

Ahmad, S., Irons, B. M., Zienkiewicz, O. C., 1970, “Analysis of thick and thin shell structures by curved finite elements”, International Journal for Numerical Methods in Engineering, Vol. 2, pp. 419-451.

Arnold, D. N., Brezzi, F., 1993, “Locking free finite elements for shells.”, ITALIA, Istituto di Analisi Numerica del Consiglio Nazionale Delle Ricerche, Pavia. Pubblicazioni N. 898, pp.1-13.

Bucalem, M. L., Nóbrega, S. H. S., 2000, “A mixed formulation for general triangular isoparametric shell elements based on the degenerated solid approach.”, Computer & Structures, Vol. 78, No. 1-3, pp. 35-44.

Cook, R., 1987, “A plane hybrid element with rotational d.o.f. and adjustable stiffness.”, International Journal for Numerical Methods in Engineering, Vol.24, pp.1499-1508.

Duarte, C.A, Babuska, I., Oden, J.T., 2000, “Generalized finite element methods for three-dimensional structural mechanics problems.”, Computer & Structures, Vol. 77, No. 2, pp.215-232.

Nóbrega, S.H.S. 1997, “Sobre o desenvolvimento de elementos finitos de casca. uma classe de formulações mistas.”, 100p. Thesis in Structural Engineering, Escola Politécnica, Universidade de São Paulo.

Nóbrega, S. H. S., Proença, S. P. B., 2004, “Locking free shell finite element: an alternative using the generalized finite element method.”, XXV CILAMCE – Iberain Latin American Congress on Computational Methods in Engineering, November 10-12, Pernambuco, Brazil, CD-ROM.

Timoshenko. S. P., Krieger, S. W., 1959, Theory of plates and shells, McGraw-Hill.

8. Responsibility notice

The authors are the only responsible for the printed material included in this paper.